Available online at www.sciencedirect.com
ScienceDirect
Journal of Hazardous Materials 157 (2008) 146–153
Journal of Hazardous Materials
www.elsevier.com/locate/jhazmat

Improvement of ground granulated blast furnace slag on stabilization/solidification of simulated mercury-doped wastes in chemically bonded phosphate ceramics

Zhongzhe Liu, Guangren Qian *, Jizhi Zhou, Chuanhua Li, Yunfeng Xu, Zhe Qin

School of Environmental Engineering, Shanghai University, Shanghai 200072, PR China

Received 6 April 2007; received in revised form 1 November 2007; accepted 26 December 2007
Available online 12 January 2008

Abstract

This paper investigated the effectiveness of (ground granulated blast furnace slag) GGBFS-added chemically bonded phosphate ceramic (CBPC) matrix on the stabilization/solidification (S/S) of mercury chloride and simulated mercury-bearing light bulbs (SMLB). The results showed that the maximal compressive strength was achieved when 15% and 10% ground GGBFS was added for $HgCl_2$-doped and SMLB-doped CBPC matrices, respectively. The S/S performances of GGBFS-added matrices were significantly better than non-additive matrices. As pore size was reduced, the leaching concentration of Hg^{2+} from GGBFS-added CBPC matrix could be reduced from 697 μg/L to about 3 μg/L when treating $HgCl_2$. Meanwhile, the main hydrating product of GGBFS-added matrices was still $MgKPO_4{\cdot}6H_2O$. The improvement of S/S effectiveness was mainly due to physical filling of fine GGBFS particles and microencapsulation of chemical cementing gel.

Keywords: Mercury-doped wastes; Stabilization/solidification; Ground granulated blast furnace slag; Chemically bonded phosphate ceramics

1. Introduction

Mercury-contaminated wastes are considered as hazardous wastes, because mercury has high toxicity, volatility and environmental mobility. Mercury exposure at high levels has both adverse effects on humans and ecosystem. Particularly for human being's health, it can harm the brain, heart and immune system. With mercury-contaminated wastes increasing, the potential risks become larger. Thus, the development of effective treatment technologies for these wastes is still a significant practical challenge for us. In China, there are about 400 million fluorescent light bulbs to be consumed every year, with 12 tonnes mercury used. Hence, safe disposal of these wastes is also an urgent problem.

Under the current regulations, such as USEPA Land Disposal Restrictions program, in the case of treating wastes with less than 260 mg/kg of mercury, such as mercury-contaminated light bulbs, the immobilization pretreatment technologies of stabilization/solidification (S/S) may be considered [1]. Among many S/S technologies, the S/S performance of chemically bonded phosphate ceramics (CBPC) technology has been demonstrated well. Compared with the traditional cement grout based S/S technologies, waste loading of CBPC is higher and the treating process can be implemented under the room-temperature without causing mercury to volatilize [2].

CBPC is a dense and insoluble ceramic matrix of magnesium potassium phosphate hydrate and is usually fabricated by the reaction below [3]:

$$MgO + KH_2PO_4 + 5H_2O \rightarrow MgKPO_4{\cdot}6H_2O(MKP) \quad (1)$$

When treating mercury-contaminated wastes, the mercury is stabilized chemically to form relatively insoluble phosphate, such as mercury phosphate, and encapsulated physically in the compact crystalline matrix of MKP.

To enhance the physical encapsulation abilities of CBPC for mercury-contaminated wastes and to reduce the practical operation costs, other binders and additives were used to substitute traditional raw binders [4]. Iron oxides (hematite and magnetite)

* Corresponding author. Tel.: +86 21 5633 8094; fax: +86 21 5633 8094.
E-mail address: grqian@shu.edu.cn (G. Qian).

0304-3894/$ – see front matter © 2008 Elsevier B.V. All rights reserved.
doi:10.1016/j.jhazmat.2007.12.110

from iron and steel industry were used as binders to replace MgO to form MKP matrix [5]. Fly ash, cement kiln dust, lime kiln dust and other industrial inorganic wastes were used as filler materials in CBPC system [6]. It was reported that fly ash as an additive can significantly improve chemical bonding of CBPC matrix with higher compressive strength and less leaching concentration of Cd, Pb, Hg and Ce [7].

Like fly ash, ground granulated blast furnace slag (GGBFS), usually used as a pozzolanic admixture in cement [8], is a granular material and possesses a fine particle size distribution with larger specific surface area. The chemical composition of GGBFS is usually rich in CaO and SiO_2. GGBFS has been proved to be a fine additive in cement hydrate system. Therefore, it was also expected that GGBFS would be beneficial to improve the physical and chemical encapsulation of mercury-bearing CBPC matrixes, by physical filling and chemical microencapsulation. Besides S/S performance being strengthened, the addition of GGBFS would occupy a considerable percentage of CBPC system, so it was also expected that the amount of raw binders would be reduced and the cost would be cut down.

In this study, GGBFS was used as an additive to enhance the S/S performances on simulated mercury-doped waste after the pretreatment of sulfide, and the improvement of GGBFS on the S/S properties of simulated mercury-doped wastes in CBPCs was investigated.

2. Experimental

2.1. Materials

MgO was obtained from Shanghai Tongya Chemical Co., Ltd. To reduce its reaction reactivity with phosphate in water, it was calcined for 4 h at 800 °C before the reaction [9]. Because of high reactivity of MgO, a very small amount of boric acid (<1% of the total powder) was used as a retardant [10]. The KH_2PO_4 was obtained from Guangdong Guanghua Chemical Factory Co., Ltd. The analytical reagent $HgCl_2$ was from Shanghai Jiachuan Chemical Co., Ltd.

The simulated mercury-bearing light bulbs (SMLB) was produced by mixing pulverized glass (≤1 mm in diameter) with certain amount of mercury chloride to make the mercury concentration constant at 200 ppm (mg/kg) which simulated the true crushed mercury-contaminated light bulbs.

The GGBFS selected in this experimentation was provided by Shanghai Baosteel Co., Ltd., the major chemical compositions of which were 41.25% CaO, 32.56% SiO_2 and 9.02% Al_2O_3.

2.2. Experiment methods

In this experiment, the content of materials was presented by weight. The content of mercury chloride was fixed at 0.25% in samples A and the loading of crushed SMLB in samples B was fixed at 40%, and all of the substances were first mixed with K_2S (≤1%) in little amount of water to form mercury sulfide. Then the stoichiometrically blended mixture (GGBFS, MgO, KH_2PO_4 and boric acid) was added and stirred together in water. After the mixture slurry was blended sufficiently, it was transferred into a plastic mold (3 cm diameter, 4 cm height) to fabricate the CBPC. These samples were characterized after completely cured for 3 weeks [11]. The detailed mixing proportion of each sample was listed in Table 1.

Table 1
Different mixing proportion (dry wt.%)

	Sample	MgO (%)	KH_2PO_4 (%)	GGBFS (%)	SMLB (%)
For S/S $HgCl_2$ matrix	A-00	22.7	77.3	0	0
	A-05	21.6	73.4	5	0
	A-10	20.5	69.5	10	0
	A-15	19.3	65.7	15	0
	A-20	18.2	61.8	20	0
	A-25	17	58	25	0
	A-30	15.9	54.1	30	0
For S/S SMLB matrix	B-00	13.6	46.4	0	40
	B-05	12.5	42.5	5	40
	B-10	11.4	38.6	10	40
	B-15	10.2	34.8	15	40
	B-20	9.1	30.9	20	40
	B-25	8	27	25	40
	B-30	6.8	23.2	30	40

2.3. Particle size distribution analysis of GGBFS

The specific surface of GGBFS was 530 m^2/kg by Blaine Air Permeability Apparatus according to GB/T 8074–1987. The particle size distribution of GGBFS was analyzed by Malver Mastersizer 2000 analyzer, based on the principle of laser diffraction in the range of 0.02–2000 μm.

2.4. Temperature rise during setting

In order to study the rate of heat evolution, which reflected the reaction kinetics, the temperature rise in the slurry was recorded by a common thermometer with a precision of ±1 °C. Simultaneously, the time of temperature rise was recorded by a digital stopwatch.

2.5. Compressive strength

The compressive strength of all samples, cured for 1, 3, 7, 14 and 21 days, were measured by a TYE-50 pressuring and bending machine produced by Wuxi Jianyi apparatus Co., Ltd.

2.6. Toxic characteristic leaching procedure (TCLP)

The USEPA TCLP method [12] was performed to determine the leaching characteristics of Hg^{2+} from CBPC samples, which reflected the S/S effect of CBPC form with GGBFS additive compared with the matrix without additive. According to the standard, the solution having pH of 2.88 ± 0.05 was chosen as the extraction liquid in this study. The concentration of the leachate was analyzed by a F732-V type cold atomic absorption analyzer of mercury obtained from Shanghai Huaguang apparatus Co., Ltd. All the TCLP results were

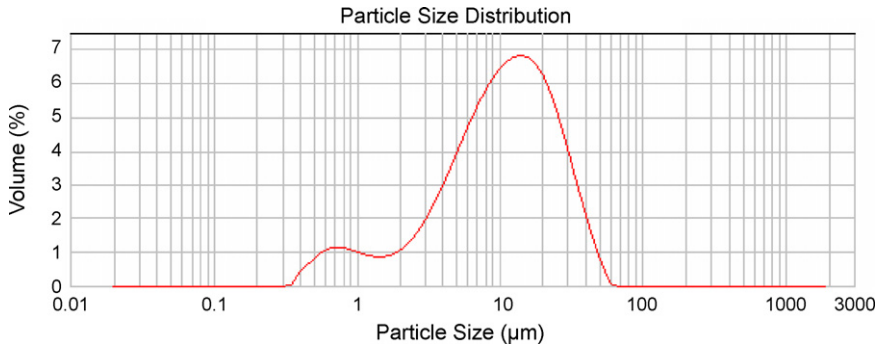

Fig. 1. Particle distribution of GGBFS.

also compared with the concentration limits allowed for landfill set by USEPA.

2.7. Porosity and pore distribution

Mercury Intrusion Porosimetry analysis was performed on the samples by a Quantachrome Pore Master Autoscan-60 to examine the pore volume and the distribution of pore sizes.

2.8. Characteristics of reaction products

2.8.1. Powder X-ray diffraction (XRD) analysis

The crystal phases in the samples were identified using a D8 Advance X-ray Diffractometer of Germany BRUKER/AXS Co., Ltd. with Cu Kα radiation 34 kV, 20 mA. After the diffraction pattern was recorded, the crystalline compounds were determined through manual matching and computer system aiding, which was presented by an intensity–2θ format.

2.8.2. Infrared spectroscopy analysis

To identify various functional groups in the chemical structures of the CBPC matrix, the infrared spectroscopy analysis was performed by a PerkinElmer 1725X Fourier transform infrared spectrophotometer. The spectral measurement in the 400–4000 cm^{-1} region was made at 4 cm^{-1} resolution with the use of 120 scans.

2.8.3. Scanning electron microscope (SEM) analysis

The surface morphologies of matrices were visualized via a JEOL JSM-6700F scanning electron microscope to analyze the difference of microstructure between GGBFS-added MKP matrix and non-additive MKP matrix.

3. Results and discussion

3.1. Particle size distribution of GGBFS

Due to the strong influence of particle size of GGBFS on the hydraulic reactivity and the compressive strength for solidified matrixes, the obtained GGBFS had been pulverized to improve its reactivity [13]. Like GGBFS as an additive used in cement, for CBPC matrices, the fineness of GGBFS was also a very important index to affect the properties of CBPC matrices.

The particle size distribution curve of GGBFS was presented in Fig. 1. The majority of GGBFS particle sizes were in the range of 0.5–50 μm, which could play a role of physical filling and might also have more rapid rate of hydration in the slurry.

3.2. Temperature rise during setting

Fig. 2 showed the temperature rise curves of different Hg-doped slurries with and without 20% GGBFS. The setting time in the mold was about 4 min after the slurry was stirred completely for about 1 min. Although the reaction of CBPC was exothermal, the reaction temperature didn't exceed 80 °C through the hardened process of the slurry [2]. As shown in Fig. 2, final temperature for each matrix was under 75 °C in this experiment, which was safe for stabilizing volatile mercury.

In Fig. 2, all the curves showed that the temperature increased slowly in the early one minute and rose rapidly in the second minute. This temperature behavior was attributed to the fact that boric acid reacted with the acid-phosphate and formed a temporary coating of lunebergite ($Mg_3(PO_4)\cdot B_2O_3\cdot 8H_2O$) on the surface of oxide particles which prevented the dissolution of MgO into the solution [14]. After the coating was dissolved and the oxide particle surface was exposed to the acid solution, the hydration rate was accelerated and more heat was evolved. Finally, the rise trend became flat and started to decrease.

As shown in Fig. 2, the temperature of sample A-00 rose up to 71 °C. However, the temperature of sample A-20 only

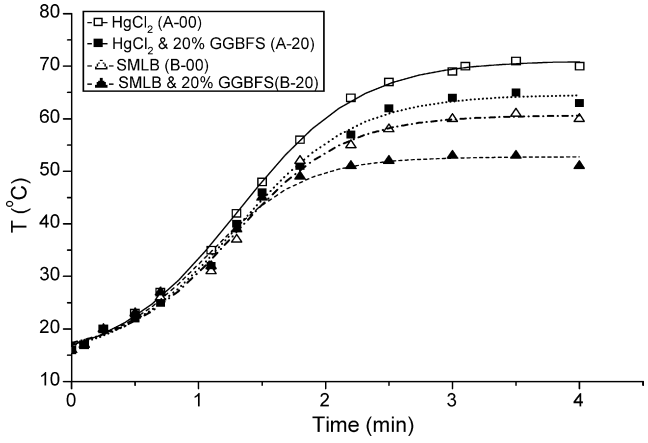

Fig. 2. Temperature rising during hydration of CBPC matrices with time.

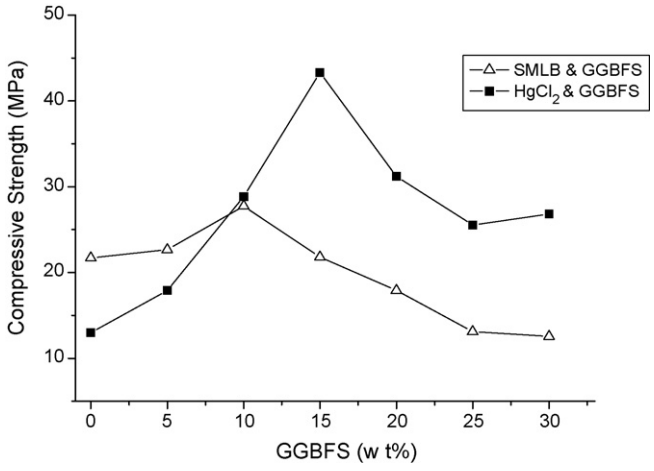

Fig. 3. Compressive strength of CBPC matrices as a function of the amount of GGBFS after 21 days.

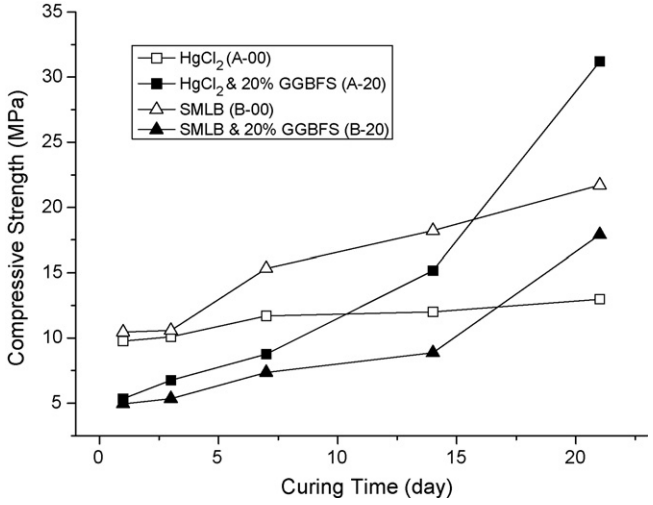

Fig. 4. Compressive strength of CBPC matrices with curing time.

reached 65 °C. Also, in the case of stabilizing SMLB, the highest temperature of sample B-20 was 8 °C lower than that of B-00, which inferred that GGBFS could reduce the total heat evolution of CBPC system. The decrease of heat evolution was most likely due to the influence on the MKP formation by the GGBFS added, which affected the hydration between MgO and KH_2PO_4.

3.3. Compressive strength

There are a lot of recommended minimum compressive strengths required for solid waste disposal at landfills [15]. In this study, the adopted criterion of compressive strength for CBPC matrices was >500 psi (3.45 MPa) as recommended by the US Nuclear Regulatory Commission Standard [16]. After cured for about 21 days, the final compressive strength with different GGBFS contents was measured and presented in Fig. 3. In the case of stabilizing $HgCl_2$, it could be observed that all the compressive strengths of samples containing GGBFS were higher than that of non-additive samples, showing that the addition of GGBFS would absolutely enhance the strengths of matrixes. Especially, the sample with 15% GGBFS possessed the highest strength, which was 43.3 MPa. When stabilizing SMLB, the highest strength occurred at 10% GGBFS content, which was 27.8 MPa. With the increasing GGBFS content, the strength of matrixes decreased gradually, attaining a lower strength value than that of the non-additive sample since 15% GGBFS added. However, no matter the amount of GGBFS added, all the compressive strength was beyond 3.45 MPa recommended by the standard.

The specimens A-20 and B-20 were chosen to trace the development of the compressive strength with time. In Fig. 4, it was shown that after cured for 1 day, A-00 and B-00 (without GGBFS) achieved the compressive strength of 10 MPa while A-20 and B-20 (with 20% GGBFS) got 5 MPa. After cured for 10 days, the strength of A-20 rapidly increased and exceeded that of A-00, while the strength of B-20 was always lower than that of B-00 even after more curing time.

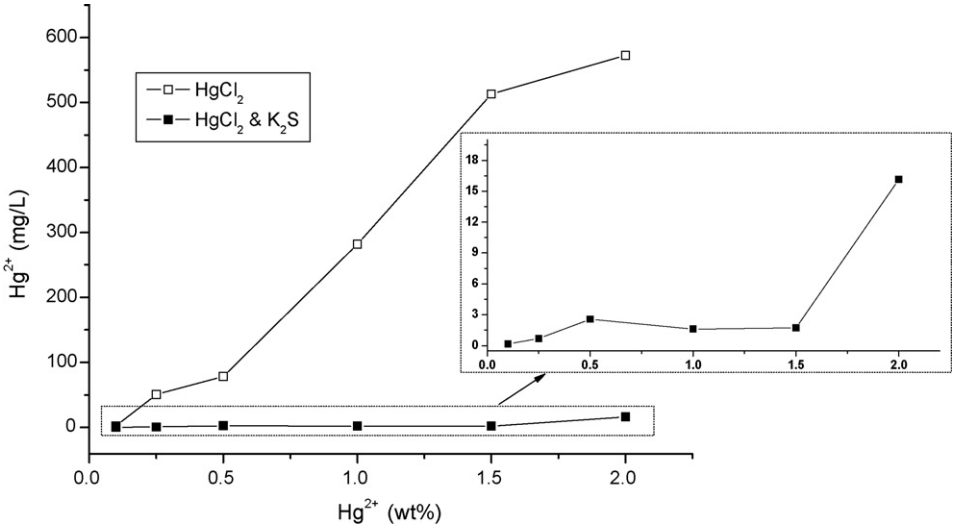

Fig. 5. Leaching of Hg^{2+} from CBPC matrices pretreated and not pretreated by K_2S.

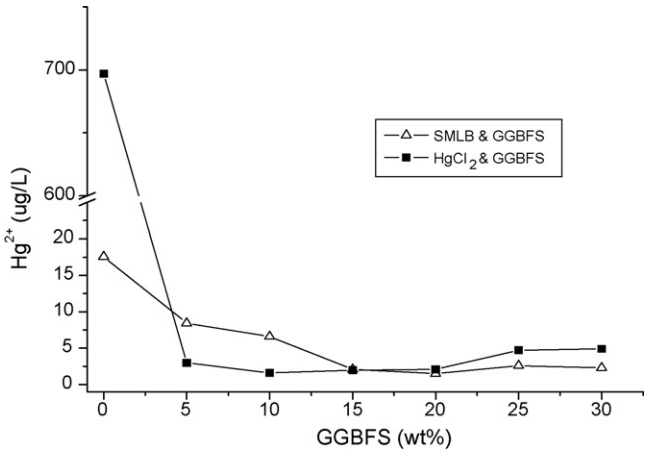

Fig. 6. Leaching of Hg^{2+} from CBPC matrices as a function of the amount of GGBFS.

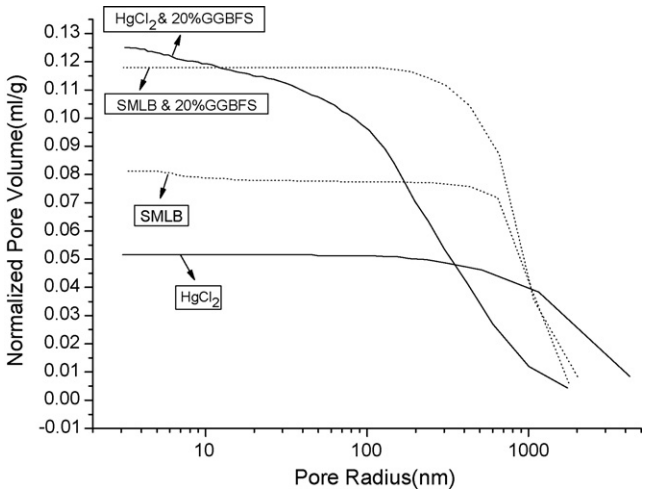

Fig. 7. Normalized pore volume versus pore radius.

3.4. Leaching behavior

The leaching behavior of all CBPC matrixes was determined according to the USEPA TCLP test procedure. Addition of a small amount (<1 wt.%) of sulfide like K_2S in the binder mixture was recommended to get a better stabilization performance [2,17]. From Fig. 5, it could be seen that, regardless of the amount of initial Hg^{2+}-loaded, the Hg^{2+} leaching concentrations of samples pretreated by K_2S were lower than that of non-pretreated ones even at high initial Hg^{2+} concentration. For initial 1%, 1.5% and 2% loading samples, the Hg^{2+} leaching concentrations were reduced from 281.8 mg/L, 512.9 mg/L, 572.7 mg/L to 1.6 mg/L, 1.72 mg/L and 16.12 mg/L, respectively, indicating the better stabilization performance of matrixes pretreated by K_2S.

The influence of the addition of GGBFS into Hg^{2+}-loaded CBPC matrixes on suppressing Hg^{2+} leaching was further studied. As seen in Fig. 6, for stabilizing $HgCl_2$, the effectiveness of adding GGBFS was quite evident. As 5% GGBFS was added, the Hg^{2+} concentration decreased dramatically from 697.08 μg/L to 2.99 μg/L. While for stabilizing SMLB, the Hg^{2+} leaching concentrations were also reduced by adding GGBFS and decreased from 17.59 μg/L to 1.5 μg/L at 20% GGBFS addition. Fig. 6 indicated that all the Hg^{2+} leaching concentration of CBPC matrices met the Universal Treatment Standard, 0.025 mg/L or less prior to disposal in a landfill [18].

3.5. Porosity and pore distribution analysis

Pore structure is important to the mechanical and leaching properties of S/S matrix. Pore volume and critical pore size are usually indicators of the microstructure. In Fig. 7, after 20% GGBFS added, the normalized pore volume of additive sample was higher than that of non-additive sample, both for S/S $HgCl_2$ and SMLB, the largest cumulative pore volume of which was increased from 0.05 mL/g, 0.08 mL/g to 0.13 mL/g and 0.12 mL/g, respectively.

Though the porosity increased, the pore size distribution tended to be finer due to the addition of GGBFS. In Fig. 8, when

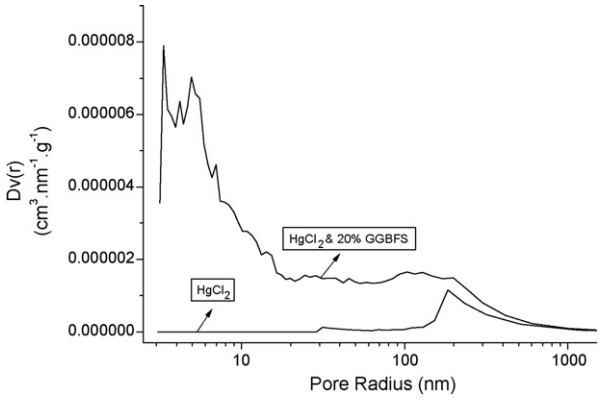

Fig. 8. Pore size distribution of S/S $HgCl_2$ samples.

treating $HgCl_2$, it was shown that three evident peaks appeared at 4.93 nm, 4.19 nm and 3.33 nm, respectively. After addition of GGBFS, the critical pore size was reduced from 183.9 nm to the minimal 3.33 nm. This dramatic change was reflected by the higher compressive strength and lower leaching performance of the samples with GGBFS. In Fig. 9, in the case of S/S SMLB, before adding GGBFS, only one peak was shown and

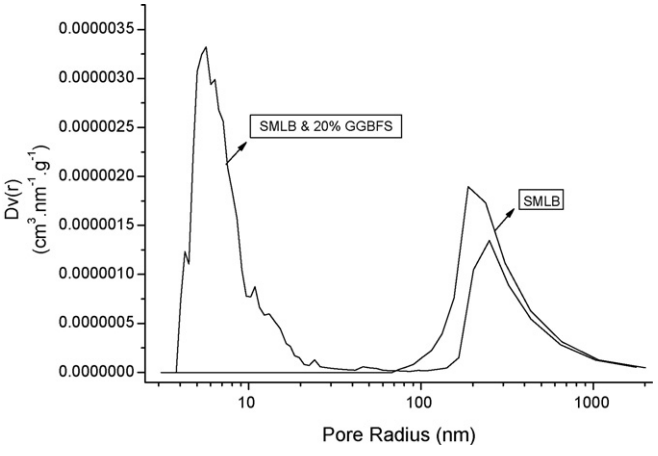

Fig. 9. Pore size distribution of S/S SMLB samples.

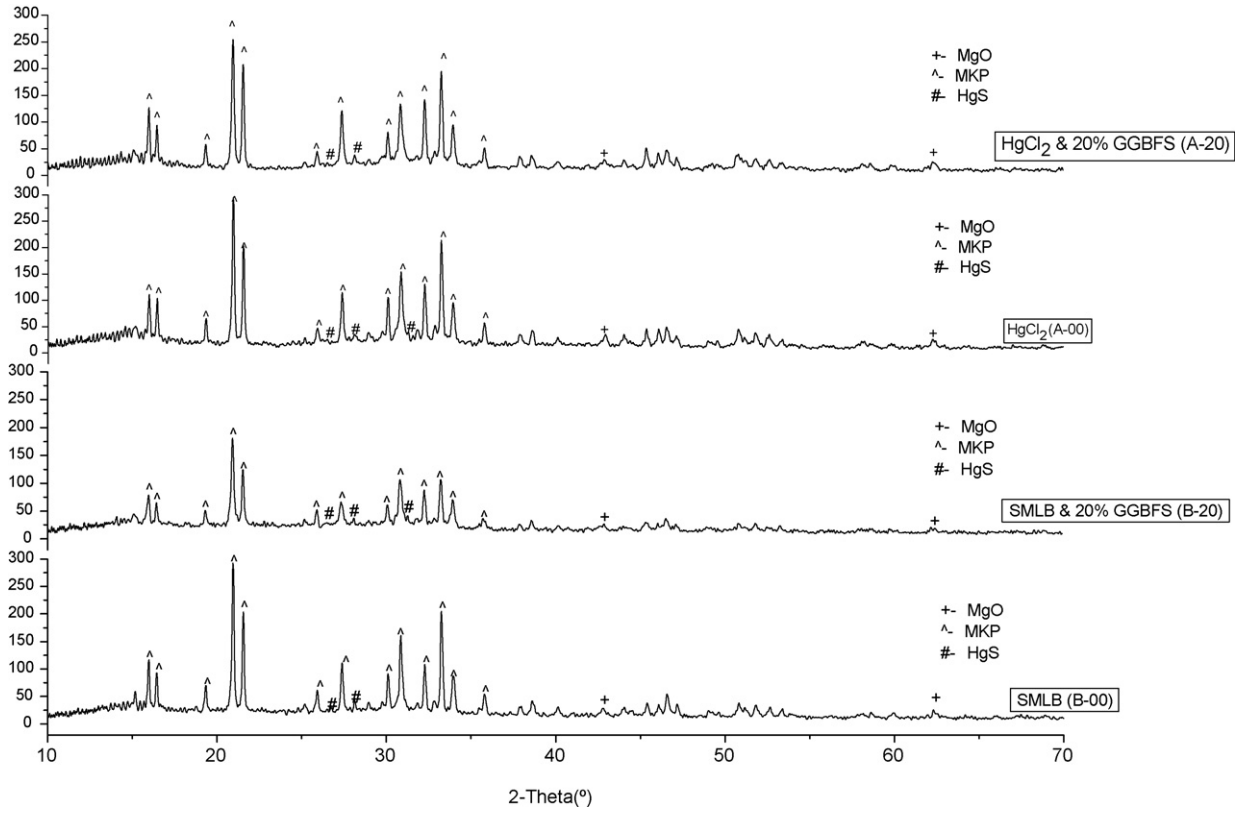

Fig. 10. X-ray diffraction patterns of CBPC samples with and without GGBFS.

the critical pore size was 188.11 nm. However, after GGBFS was added, it could be seen that the matrices possessed two peaks, one critical pore size of which was 5.65 nm, indicating that the previous critical pore size was also reduced significantly, similar to treating $HgCl_2$. Therefore, it could be inferred that the S/S effectiveness of GGBFS-added SMLB matrices was also well related with the improvement of micropore distribution.

3.6. Characterization of reaction products in S/S matrix

3.6.1. XRD analysis

The specimens A-20 and B-20 were selected to identify the reaction products formed in GGBFS–CBPC matrixes by XRD analysis, compared with the matrices A-00 and B-00. In Fig. 10, three strongest lines of magnesium potassium phosphate hexahydrate ($MgKPO_4{\cdot}6H_2O$) crystal were mainly in the locations of $d = 4.24$ Å, 4.12 Å, 2.90 Å. The traces of cinnabar (HgS) appeared at 3.36 Å, 3.17 Å and 2.87 Å, which suggested that the stabilization of Hg^{2+} in CPBC matrix was partly due to the formation of insoluble mercury sulfide. Some residual periclase (MgO) was also found in the XRD pattern, located at 2.11 Å, 1.49 Å. Due to GGBFS being amorphous and vitreous, the amorphous species were difficult to be identified by XRD.

The diffraction intensity reflected the amount of crystalline phases to some extent. From the intensity–2θ format, it showed that MKP diffraction intensity of the sample without GGBFS was obviously higher than that with 20% GGBFS. It implied that the addition of GGBFS would decrease the amount of well crystallized MKP phase.

From the XRD results above, despite some differences in intensity, there was no new crystalline phase formed and the main crystal phase of all the samples was still MKP after the addition of GGBFS. This showed that the addition of GGBFS had no obvious influence on the formation of major crystalline phase MKP.

3.6.2. FTIR analysis

The micro-surrounding of S/S matrix structure was characterized by Fourier transform infrared (FTIR) spectrum. The spectra of the four samples were shown in Fig. 11. The absorption band 2982–2979 cm^{-1} was ascribed to the O–H stretching of H_2O. At 2376–2372 cm^{-1}, it was due to the hydrogen bond ((*p*)–O–H stretching). The other band of adsorption H_2O was at 1632–1631 cm^{-1}, which was a bend vibration. At 1492–1424 cm^{-1} and 749–746 cm^{-1}, asymmetric stretching vibration and bend vibration were all due to CO_3^{2-}. The absorption band 1013–1012 cm^{-1} and 573–572 cm^{-1} were attributed to PO_4^{3-} ($V_3(PO_4)$). The band at 790 cm^{-1} was the bend vibration of Al–O–Si bond.

From FTIR results, it was noticed that a new evident absorption band appeared at 790 cm^{-1} in specimens A-20 and B-20, which was caused by Al–O–Si bond, after GGBFS was added. The CO_3^{2-} present was most likely from the impurity in MgO during its production. For A-20 and B-20, it was

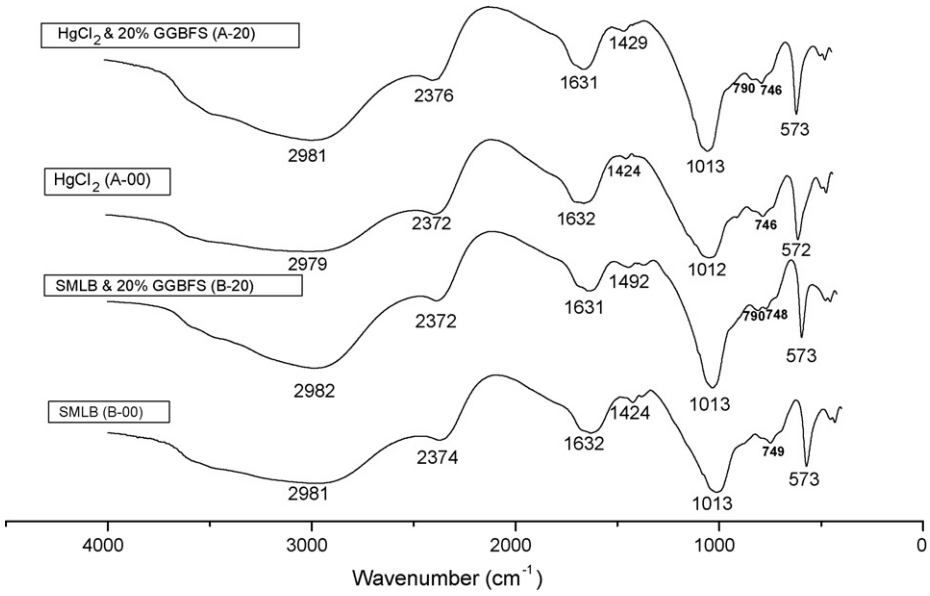

Fig. 11. IR-spectra of CBPC matrices with and without GGBFS.

shown that the addition of GGBFS made CO_3^{2-} absorption bands widened to higher frequency, but had no evident effect on PO_4^{3-}. Therefore, it could be concluded that the crystallite of MKP was not deformed or disordered by importing GGBFS.

3.6.3. SEM analysis

The SEM analysis was used to have a deeper insight into the S/S mechanism. In Fig. 12a, the microstructure of MKP without GGBFS consisted of larger quantities of short rod-like crystalline phases. From Fig. 12b, it was shown that, after 20% GGBFS was added, the previous well crystallized phases almost disappeared or blurred. There were lots of amorphous gel-like hydrates surrounding the blurred MKP crystals, and these gel-like hydrates were mostly embedded in the matrix, filling gaps or pores. Consequently, it was inferred that this cementitious gel improved S/S effects of CBPC matrixes.

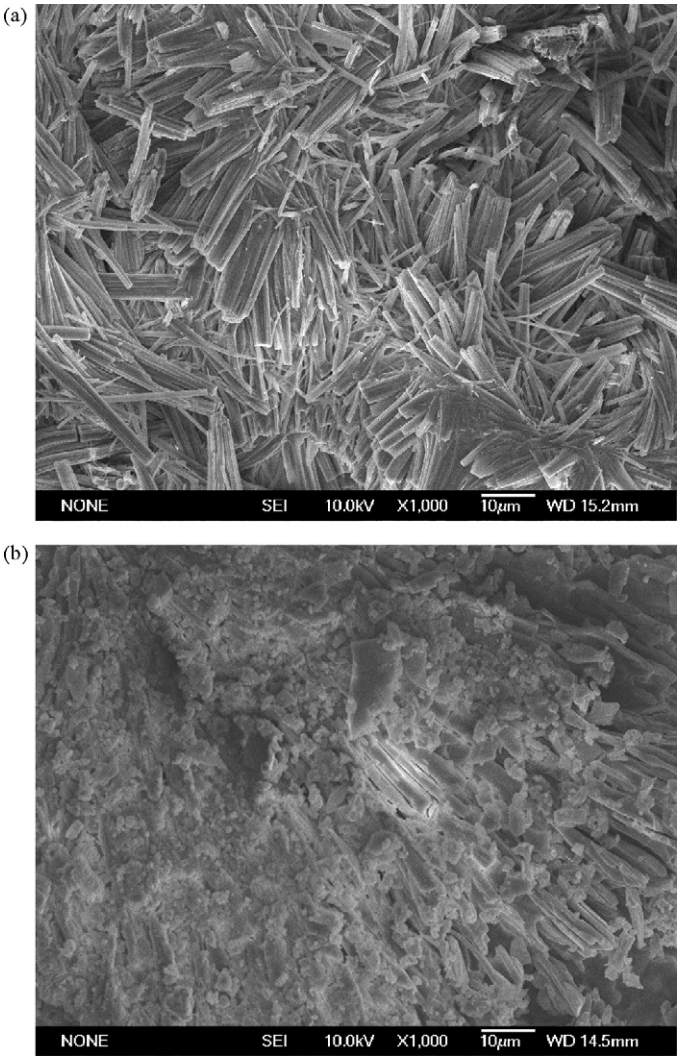

Fig. 12. SEM photographs of MKP matrices (a) without GGBFS (b) with 20% GGBFS.

3.7. Discussion

Based on the results above, the functions of GGBFS for reinforcing S/S of Hg-bearing CBPC matrixes could be assumed as physical filling by fine GGBFS particles and microencapsulation by cementing gel formed by GGBFS and phosphate.

From the XRD and FTIR results, the addition of GGBFS had no influence on the formation of $MgKPO_4{\cdot}6H_2O$ and the bond of PO_4^{3-}. The main crystal phase was still MKP. Thus, GGBFS and potential formed gel mainly played the role of filling the voids of the matrix. Appropriate amount of GGBFS added would be beneficial for both leaching performance and compressive strength to reach an optimum packing.

On the other hand, Willson established that aluminosilicate glass could react with phosphoric acid to form a strong phosphate bonded cement material, which was believed to be aluminum phosphate gel (other than silicate gel) [19]. Furthermore, for

fly ash-added CBPC system, the formation of aluminum phosphate gel was also assured by the reaction between aluminum phosphate solution and aluminosilciates contained in fly ash [20]. Like fly ash, GGBFS is also a glassy amorphous material containing CaO, SiO_2 and Al_2O_3. As proven in the SEM micrographs, when GGBFS was blended into the CBPC system, some ions such as Ca^{2+}, Al^{3+} might be disassociated from aluminosilicate glass and formed aluminum phosphate gel with phosphates by hydration reaction. Furthermore, to testify if any reaction did occur between GGBFS and KH_2PO_4 solution, the two were mixed and cast in the mold, and it was found that the product was a firmly hardened mass after about 10 days. This indicated that the cementitious gel could also form in this GGBFS-added CBPC system. The formed gel could act as a pozzolanic admixture, making the matrix denser and the pore structure finer to achieve better compressive strength and lesser Hg^{2+} leaching performance, microencapsulating the mercury-contaminated wastes more tightly.

4. Conclusions

This study showed that ground granular blast furnace slag had obvious improving effectiveness on stabilizing and solidifying mercury-doped CBPC matrixes as follows:

1. The addition of GGBFS significantly reduced Hg^{2+} leaching concentration and enhanced compressive strength of mercury-doped CBPC matrixes.
2. The addition of GGBFS made the pore structure of mercury-doped CBPC matrixes finer by reducing its critical pore size.
3. The addition of GGBFS could also refrain from the reaction temperature rise of matrix to prevent the volatilization of mercury.
4. Both physical filling of GGBFS and microencapsulation of cementing gel were responsible for less leaching and better physical performances of mercury-doped CBPC matrixes.

Acknowledgements

This project was supported by 2004 National Nature Science Foundation of China No.20477024, 2007 National Nature Science Foundation of China No.20677037, 2005 Shanghai Key Education Research Fund (TD105).

References

[1] S. Chattopadhyay, Evaluation of chemically bonded phosphate ceramics for mercury stabilization of a mixed synthetic waste, EPA/600/R-03/113 (2003).
[2] Stabilization using phosphate bonded ceramics, U.S. Innovative Technology Summary Report, DOE/EM-0486, 1999.
[3] A.S. Wagh, D. Singh, S.Y. Jeong, Chemically Bonded Phosphate Ceramics for Stabilization and Solidification of Mixed Waste, Encyclopedia of Environmental Technology, CRC Press, 2001, pp. 6.3-1–16.3-18.
[4] J.R. Conner, S.L. Hoeffner, The history of stabilization/solidification technology, Crit. Rev. Env. Sci. Tec. 28 (1998) 325–396.
[5] A.S. Wagh, S.Y. Jeong, D. Singh, A.S. Aloy, T.I. Kolytcheva, E.N. Kovarskaya, Y. Macheret, Iron-phosphate-based chemically bonded phostphate ceramics for mixed waste stabilization, in: Waste Management Annual Meeting, Tucson, AZ, March, 1997.
[6] S. Chattopadhyay, W.E. Condit, Advances in encapsulation technologies for the management of mercury-contaminated hazardous wastes, EPA Technical Report, 2002.
[7] S. Bannerjee, Utilization of fly ash in construction by improved chemical bonding, in: Third Conference on Unburned Carbon on Utility Fly Ash, National Energy Technology Laboratory, 1997.
[8] T. Hakkinen, The influence of slag content on the microstructure, permeability and mechanical properties of concrete. Part 1, Cem. Conc. Res. 23 (1993) 407–421.
[9] A.S. Wagh, R. Strain, S.Y. Jeong, D. Reed, T. Krause, D. Singh, Stabilization of rocky flats Pu-contaminated ash within chemically bonded phosphate ceramics, J. Nucl. Mater. 265 (1999) 295–307.
[10] P. Randall, S. Chattopadhyay, Advances in encapsulation technologies for the management of mercury-contaminated hazardous wastes, J. Hazard. Mater. 114 (2004) 211–233.
[11] A.S. Wagh, D. Singh, S.Y. Jeong, Mercury stabilization in chemically bonded phosphate ceramics, in: Environmental Protection Agency's Workshop on Mercury Products, Processes, Waste, and the Environment: Eliminating, Reducing and Managing Risks, Baltimore, MD, March, 2000.
[12] USEPA Method 1311, Toxicity Characteristic Leaching Procedure.
[13] S. Song, D. Sohn, H.M. Jennings, T.O. Mason, Hydration of alkali-activated ground granulated blast furnace slag, J. Mater. Sci. 35 (2000) 249–257.
[14] A.S. Wagh, S.Y. Jeong, Cementing the gap between ceramics, cements, and polymers, Mater. Technol. 18 (2003) 162–168.
[15] M.D. Grega, Hazardous Waste Management, McGraw-Hill International Edition, 2001.
[16] ASTM Standards, Standard Test Method for Normal Consistency of Hydraulic Cement, vol. C187–83, ASTM Designation, 1983, pp. 195.
[17] D. Singh, A. Wagh, J. Cunnane, J. Mayberry, Chemically bonded phosphate ceramics for low-level mixed-waste stabilization, J. Environ. Sci. Heal. A32 (1997) 527–541.
[18] USEPA 40 CFR Part 268 for Treated Wastes, 1994.
[19] W.A. Wilson, J.W. Nicholson, Acid-Base Cement. Their Biomedical and Industrial Applications, Cambridge University Press, 1993, p. 204.
[20] T.L. Demirel, D.-Y. Lee, M. Boybay, Process of producing hydraulic cement from fly ash, US Patent 4328037 (May 4, 1982) 5.